

Original Research

Spatial Land Use Optimization Using the CLUE-S Model: a Case Study in the Keerqinzuoyihou Banner, China

Yufeng Zhang¹, Mingkai Yu^{2*}, Yuansen Ye^{1**}

¹College of Geographical Science Inner Mongolia Normal University Hohhot, China

²Inner Mongolia third Geology and Mineral Exploration and Development Co., LTD Hohhot, China

Received: 25 February 2022

Accepted: 5 July 2022

Abstract

Structural contradictions among cities, agriculture, animal husbandry, and ecosystems in agriculture/pastoral zones have become increasingly prominent. This study analyzed land use change for a typical farming-pastoral interlacing area in the Keerqinzuoyihou Banner, China, using land use status data from 2009 to 2017. The drivers of land use changes were determined using logistic regression analysis. The Conversion of Land Use and its Effects at Small Region Extent (CLUE-S) model simulated four scenarios (i.e., natural evolution, ecological, economic, and social benefits maximization), and there were three key findings. First, land use structure mainly consisted of cropland, forest, and grassland; these accounted for nearly 90% of the total land area. There was a rapid increase in cultivated and built-up areas from 2009 to 2017. Second, the Kappa coefficient of the CLUE-S simulated results and actual land use was 0.936, indicating high model accuracy and applicability for simulating spatial land use distribution in the study area. Third, under the natural evolution scenario, forest, grassland, water bodies, sandy land, and unused land decreased from 2017 to 2025, whereas cropland and built-up land increased. This provides a reference to guide government land use planning and measures to improve land use efficiency and optimize the industrial structure.

Keywords: land use change, CLUE-S model, scenario simulation, optimal allocation of land use

Introduction

Land resources are important for the survival and development of human society [1]. In China, the current baseline national condition is characterized by more people and less land [2]. With the acceleration of industrialization, informatization, and urbanization,

the demand for land resources has escalated, creating an increasingly prominent mismatch between people and land. The most significant problems affecting land resources include deforestation, grassland reclamation, and the use of inefficient and extensive land use and management models to address soil erosion, declines in soil fertility/quality/carrying capacity, ecological risk intensification, and other issues [3]. Thus, the efficient, scientifically determined, and rational allocation of limited land resources is an urgent issue for local and foreign researchers alike.

*e-mail: 136839724@qq.com

**e-mail: yeyuansen@126.com

Remote sensing satellite data have become increasingly abundant (e.g., National Oceanic and Atmospheric Administration [NOAA]/Advanced Very High Resolution Radiometer [AVHRR] [4], Systeme Probatoire d'Observation de la Terre [SPOT]/Vegetation [5], Terra, Aque/Moderate-Resolution Imaging Spectroradiometer [MODIS] [6], Landsat Multispectral Scanner [MSS]/Thematic Mapper [TM]/Enhanced Thematic Mapper Plus [ETM+]/Operational Land Imager [OLI] [7], Advanced Land Observation Satellite [ALOS]/Advanced Visible and Near Infrared Radiometer Type [AVNIR] [8], and Sentinel [9]). These sources provide valuable land use information and lay the foundation for the study of regional land use change. As such, researchers have accumulated large quantities of data and research results on land-use patterns [10-11], spatio-temporal processes, driving forces, and environmental effects (ecology/soil/atmosphere) at global and regional scales. However, there is a relative lack of research on how to use these results to optimize regional land allocation under different levels of economic development. This optimization may inform decision-making related to the allocation of land resources.

Optimal land use allocation involves two parts: (1) land use structure optimization; and (2) space layout optimization. In-depth studies have been conducted on both aspects to optimize land use structures. Multiple objective functions are set to determine the optimal ratio of various land use types under different situations using historical land use change data and mathematical models [12]. Optimizing the spatial land use distribution involves reasonably allocating land use structures in space [13]. However, it has become difficult to carry out spatial land use optimization due to spatial characteristics, multiple objectives, and the diversity of land use types. Researchers have developed many spatial layout optimization algorithms, such as genetic algorithms [14-16], particle swarm optimization [17-19], the artificial immune algorithm [20], artificial fish algorithm [21], annealing algorithm [22-23], and the ca model [24-26]. These algorithms calculate the spatial layout of different economic benefit maximization scenarios; however, these methods involve lengthy processes. Compared with existing algorithms and models, the Conversion of Land Use and its Effects at Small Region Extent (CLUE-S) model demonstrates good spatial allocation ability and considers the natural and human drivers of land use change in the spatial allocation process [27]. As such, this model has been widely used to simulate various land uses including built-up urban, small-area farmland, and oasis areas. The CLUE-S model requires sufficient historical land use change information in order to provide an accurate spatio-temporal transformation relationship on land use [28].

As a part of the farming-pastoral interlacing in northern China, the Keerqinzuoyihou Banner represents

a typical ecologically fragile area that is sensitive to global climate change. From the 1960s to 1990s, large land reclamation activities have led to a significant increase in the extent of desertification. Since 1999, a series of ecological restoration projects implemented by the Chinese government have drastically altered the land use situation in northern China; agriculture and animal husbandry have become key ecological restoration projects. Many studies have investigated the spatio-temporal change process [29], driving forces [30-31], and environmental effects [32] of land use in the ecotone between agriculture and animal husbandry; however, there is still a lack of scenario-based simulations of future land use patterns. The study of land use patterns under different future scenarios is considered an effective means to understand the mutual feedback mechanism between land use systems and terrestrial ecosystems and reduce potential ecological risk from future land use processes.

This study carried out a case study in the farming-pastoral ecotone of the Keerqinzuoyihou Banner to achieve three key objectives. First, land use data obtained from ALOS satellite remote sensing data were visually interpreted to analyze land use change from 2009 to 2017 (a total of five periods). Second, to simulate spatial land use patterns in 2017 based on the CLUE-S model using land use data from 2009 to 2015, the reliability of simulation results was verified by comparing with actual land use data. Third, we predicted the natural evolution in 2025 at the land use scale using the gray prediction model. Then, the analytic hierarchy process and linear programming method were used to predict the social, ecological, and economic benefits in 2035 at this same scale. These results will help highlight ecologically fragile zones and inform optimal land use allocation in key areas, providing benefits as a reference and demonstration.

Materials and Methods

Study Area

The Keerqinzuoyihou Banner is located in the south of Tongliao City, Inner Mongolia Autonomous Region, with a spatial position between 121°30'-123°43'E and 42°40'-43°42'N, covering an area of approximately 1.15×10^4 km² (Fig. 1). The region has a temperate continental climate, with high temperatures and rain in summer and cold, dry winters. The annual average temperature is 5.8°C, the annual average precipitation is 451.1 mm, and 60%-70% of precipitation is concentrated in summer (June to August). The topography is generally high in the west and low in the east, with an altitude of 89-301 m and a slope of 0°-10.58°. The main soil types are aeolian sand and meadow soils, while alkaline, swamp, and peat soils are scattered throughout the study area.

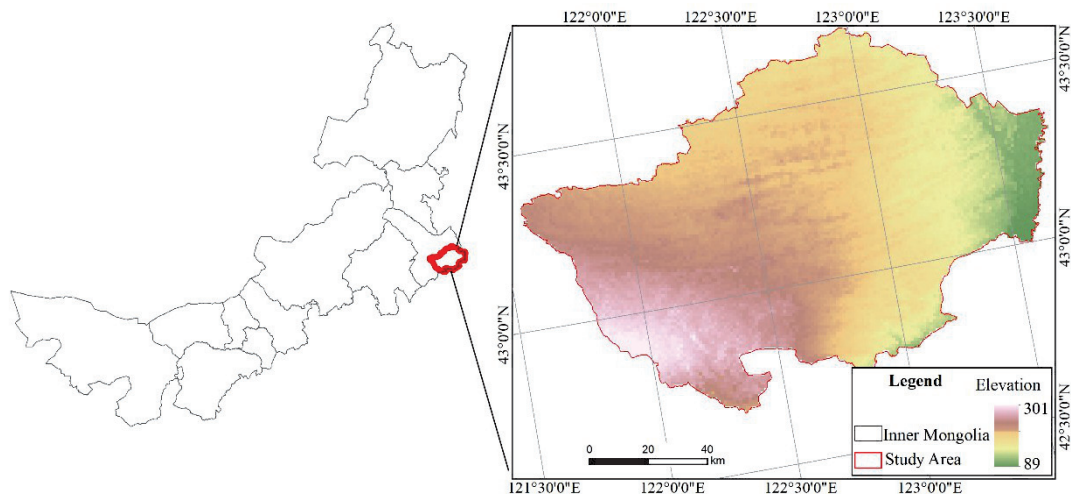


Fig. 1. Location of study area.

Data Collection and Pre-Processing

Land Use Data and Digital Elevation Model Datasets

The land use dataset was derived from the multispectral data acquired by the Avnir-2 sensor of the Japanese ALOS satellite and obtained through manual visual interpretation. Avnir-2 multispectral data consists of four bands: blue (420-500 nm), green (520-600 nm), red (610-690 nm), and near-infrared (760-890 nm); it has a spatial resolution of 10 m and an image width of 70 km. The land use data spanned from 2009 to 2017, with an interval of two years, and a total of five data periods. The accuracy of the visual interpretation was verified by field sampling points; the overall accuracy was 93.7%.

Digital elevation model (DEM) data were obtained from the Advanced Spaceborne Thermal Emission and Reflection Radiometer Global Digital Elevation Model (ASTER GDEM) dataset jointly produced by the Ministry of Economy, Trade and Industry (METI) of Japan and the National Aeronautics and Space Administration. These data may be downloaded from the Geospatial Data Cloud Platform of the Chinese Academy of Sciences (<http://www.gscloud.cn/>), with a 30 m spatial resolution.

Socio-Economic Data

The socio-economic data required for the CLUE-S model were obtained from the Statistical Yearbook of Inner Mongolia Autonomous Region, Statistical Yearbook of Tongliao City, Work Report of Keerqinzuoyihou Banner Government, and the Statistics Bureau of Inner Mongolia Autonomous Region from 2009 to 2017 (<http://tj.nmg.gov.cn/>).

Methods

The effect of the CLUE-S model on medium and small scale land use scenarios was apparent. The model consisted of two parts: non-spatial land use demand analysis, and land use spatial allocation.

Non-Spatial Land Use Demand Analysis

In this part, historical land use change within a certain period was used to obtain the quantity of different land uses in the target year; this was established as the constraint for spatial allocation. The specific calculation process involved three key steps. First, the land use changes from 2009 to 2017 were calculated. Second, the gray prediction model (GM 1.1) [33] was used to calculate the land use demand area for each land use type in 2025. Third, based on the linear programming method [34], objective functions under three scenarios maximizing social, ecological, and economic benefits [35] in 2035 were established to simulate and calculate the area required for each land use type. The benefit weight was determined by the analytic hierarchy process (AHP) method [36], and the target, criterion, and index layers were selected for each scenario.

Spatial Land Use Allocation

This part includes three processes: model parameter settings, logistic regression, and CLUE-S model calculation and testing.

The model parameters mainly include driving factors, land use transfer rules, regional constraints, land use quantity demand, and initial land use data. Direct or indirect driving factors may generate instability in land use change, particularly for the ecologically fragile Keerqinzuoyihou Banner farming-pastoral ecotone.

Nine drivers (i.e., distance from rural residential areas, distance from cities, distance from main roads, distance from main rivers, distance from reservoirs and lakes, slope, aspect, and elevation; Table 2) were selected based on the existing literature on the drivers of land use change in the arid and semi-arid areas of northern China. Using ArcGIS software for rasterization, the spatial resolution was set to 200 m.

The conversion coefficient and transfer matrix were also established for land use transfer rules. The former describes the conversion difficulty between different land use types, with a value between 0 and 1; the specific value was determined based on expert knowledge and the status quo of land use transfer in the study area from 2009 to 2017. The land use transfer matrix used a change-detection algorithm.

The regional constraint was a separate constraint on specific areas where land use change did not occur. Here, the basic cropland protection area in the

Keerqinzuoyihou Banner of Horqin was the regional constraint, set as -9998, while other areas were set as the land use change zone.

The demand value for land use included the land use demand from 2009 to 2017 and demand under different scenarios; the initial land use plan was established in 2009.

Logistic regression was used to establish the relationship between driving factors and land use types; it was determined using Equation (1):

$$\text{Log}\left(\frac{p_i}{1-p_i}\right) = \beta_0 + \beta_1 X_1 + \beta_2 X_2 + \dots + \beta_n X_n \quad (1)$$

where p_i represents the probability of each grid element appearing in a certain category; X_1-X_n represents each driver; $\beta_1, \beta_2, \dots, \beta_n$ represents the regression coefficient corresponding to each driver; and β_0 represents the constant of the regression analysis.

Table 1. Parameter settings for AHP model under different scenarios.

	Scenario		
	Social effect	Ecological benefit	Economic benefit
Target layer	Ecological benefits of land	Ecological benefits of land	Ecological benefits of land
Rule layer	The population density; park area per capita; per capita cultivated area; per capita residential area; per capita income	Green plant coverage; species richness; per capita industrial sulfur dioxide emissions; per-site industrial wastewater discharge; Investment in environmental pollution	Local retail sales of consumer goods per capita; land per capita labor input; per capita fixed assets investment; GDP per land; tax revenue per land
Index layer	Cropland, forest, grassland, built-up, water bodies, sandy land, unused land		

Table 2. Logistic regression coefficient distribution of different land use types.

Factor	Cropland	Forest	Grass-land	Built-up	Water bodies	Sandy land	Unused land
ROC value	0.735072	0.75633	0.870304	0.75633	0.871849	0.737562	0.750919
Constant	2.163326	-2.471573	-2.274552	-1.720939	-0.168546	-4.912449	-3.546635
Distance from rural settlements	-0.000646	0.000083	0.0004	-0.001057	-0.000125	0.00005	-0.000317
Distance from town	-0.00001	0.000016	0.000008	-0.00003	-0.000047	-0.000009	-0.000022
Distance from main highway	-0.000025	-0.000005	0.000012	-	-	0.000028	-
Distance from the railway	-0.000008	0.000016	-0.000004	-0.000015	-	-0.000006	0.000043
Distance from major rivers	-0.000022	-0.00002	0.000026	-0.000006	-	-0.000007	0.000039
Distance from the reservoir lake	0.000019	-	0.000009	-	-0.000804	-0.000032	-0.000102
Elevation	-0.008728	0.001791	0.00573	-	-0.007741	0.0101	-0.004538
Slope	0.13148	0.287827	-0.215791	-	-	-0.731889	0.179005
Slope direction	-0.000261	-	-	-	-	0.000424	-

Note: ‘-’ represents the factor removed after logistic regression.

Table 3. Area percentage of different land use types in the study area from 2009 to 2017.

Land use types	Area percent (%)					
	2009	2011	2013	2015	2017	Mean
Cropland	22.25	22.82	22.87	23.47	23.62	23.01
Forest	15.65	15.6	15.59	15.58	15.45	15.57
Grassland	52.09	51.54	51.49	50.89	50.87	51.38
Built-up	2.36	2.43	2.49	2.54	2.6	2.48
Water bodies	0.95	0.95	0.95	0.95	0.95	0.95
Sandy land	4.08	4.07	4.06	4.05	4.06	4.06
Unused land	2.62	2.58	2.54	2.51	2.45	2.54

Table 2 presents the regression coefficients calculated in this study. Logistic regression analysis [37] determined the contribution of each driver to land use change and predicted and simulated future changes. Regression results were verified using the receiver operating characteristic (ROC) curve [38].

Following input from all parameter files, the CLUE-S model was run to output the simulated map of the spatial land use layout in 2017 for the Keerqinzuoyihou Banner. Simulation accuracy was verified using the calculated kappa coefficient with real results; the spatial land use layout under different scenarios in 2035 was obtained based on this verification. The kappa coefficient was calculated as follows:

$$Kappa = \frac{p_0 - p_c}{1 - p_c} \quad (2)$$

where p_0 represents the correct scale to simulate; and p_c represents the correct ratio expected to be simulated in the random case.

Results and Discussion

Spatio-Temporal Changes in Land Use from 2009 to 2017

Table 3 shows the proportion of area in each land use type in the Keerqinzuoyihou Banner from 2009 to 2017. The areas of cropland (23.01%), forest (15.57%), and grassland (51.38%) accounted for 89.96% of the entire study area. The areas of built-up (2.48%), water body (0.95%), sandy land (4.06%), and unused land (2.54%) accounted for only 10.04% of the study area. Over the nine years, the cropland and built-up areas increased annually, while forest land, grassland, and unused land decreased each year; the area of water bodies and sandy land remained unchanged.

The probability transfer matrix of land use was established to more conveniently and intuitively reflect the mutual transformation among various land use types

from 2009 to 2017 (Appendix Table 1). The results show that a very small amount of cropland was transferred to built-up areas, whereas built-up areas were not transferred. Forest land, grassland, water bodies, sandy land, and unused land were all transformed into cropland and developed by the end of 2017. At this time point, only the cropland and built-up areas increased, while other land use types decreased. In addition, 0.47% of sandy land was converted to arable land, 0.06% of sandy land was converted to built-up land, and there was no transfer to other land use types. This indicates that although the Keerqinzuoyihou Banner has emphasized desertification control, the effect of this emphasis has not been significant. Unused land, as a reserve resource, decreased by 6.64% in just nine years and was mainly converted into cropland.

Fig. 2 shows that from 2009 to 2017, land use changes in the Keerqinzuoyihou Banner were mainly distributed in Ganqika, Hailutu, Jinbaotun, and Charisu towns. Among them, Ganqika, as the resident of the banner government, was a centralized distribution area for new built-up areas. New croplands were mainly distributed in Hailutu, Charisu, Jinbaotun, and Aduqinsumu towns, and mainly manifested through the conversion of grassland into cropland. The reduced area of cropland was mainly converted to built-up areas, distributed in Ganqika. The reduced area of forest was mainly converted into built-up areas, distributed in Ganqika, Jinbaotun, Aduqinsumu, and Maodao Tusumu towns. The reduced area of grassland was mainly converted into cropland, distributed in Ganqika, Jilgalang, Hailutu, Zharisu, and Aduqin Sumu towns.

Simulation Accuracy Verification of Spatial Layout of Land Use

To test the accuracy of the CLUE-S model in terms of spatial land use layout, the 2017 spatial layout was simulated based on the 2009 land use status map and compared with the actual land use status map (Appendix Fig. 1). The results show that 27617 grids were correctly simulated, accounting for 94.5% of the total number of grids (287418). In this study, seven land use types were

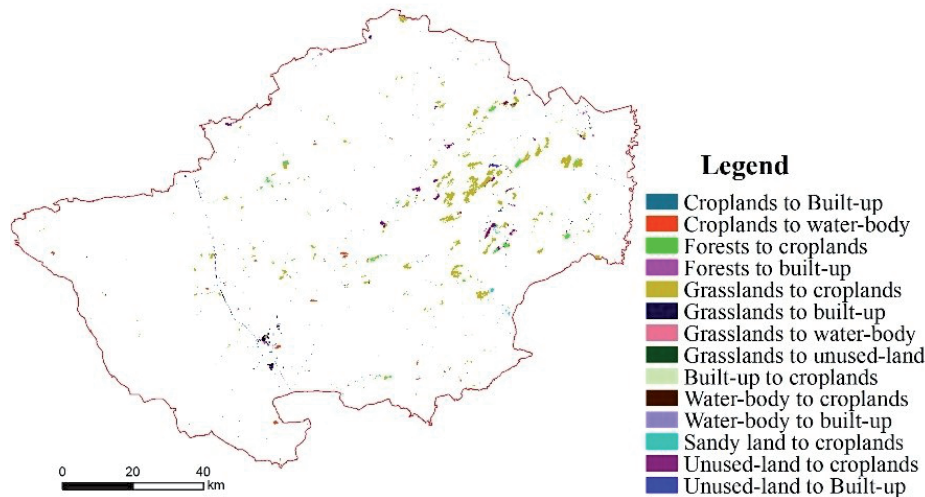


Fig. 2. Spatial distribution of land use change from 2009 to 2017.

included, and the correct simulation ratio of each type of land use grid was 1/7 in the stochastic simulation state. Therefore, the Kappa coefficient calculated by Equation (2) was 0.936, indicating high simulation accuracy that could be used to predict the spatial layout of future land use in the Keerqinzuoyihou Banner.

Multi-Scenario Simulation of Land Use Change

Natural Evolution Scenario Simulation in 2025

Under the natural evolution scenario, forest land, grassland, water body, sandy land, and unused land decreased by 2513.40, 14573.242, 24.21, 320.60 and 1834.13 hm², respectively. The cropland and built-up increasing to 16232.17 and 3033.41 hm², respectively.

The probability matrix of land use transfer was established (Appendix Table 2) to clearly present the

transfer situation among land classes. From 2017 to 2025, approximately 0.13% of cropland was converted to grassland and built-up areas, and 5.44% of the built-up area was converted to cropland. Forest land and grassland were mainly converted to arable land at 1.74% and 2.09%, respectively. Water bodies, sandy land, and unused land all changed, albeit on a smaller scale.

Fig. 3 shows that most land use change in the study area was concentrated along major highways and near major rivers and lakes. Among them, the area of increasing cropland was primarily located in Nugustai, Ganqika, Changsheng, Charisu, Hailutu, Jinbaotun, Jirigalang and Shuangsheng towns. Increased built-up areas were distributed across Nugustai, Ganqika, Changsheng, Charisu and Aduqin Sumu towns. The conversion of cropland to grassland was mainly concentrated in Charisu, Hailutu and Jinbaotun towns.

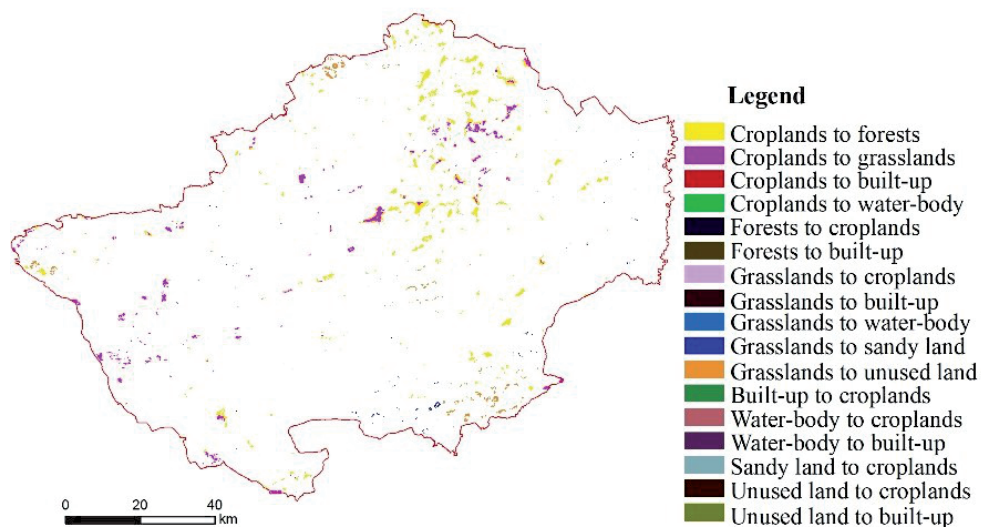


Fig. 3. Spatial land use change distribution under the natural evolution scenario for the Keerqinzuoyihou Banner from 2017 to 2025.

Scenario Simulation for Maximizing Social Benefits in 2035

Under the maximum social benefit scenario, cropland and forest will maintain the scale of 2025, while the scale of grassland, water bodies, sandy land and unused land will decrease by 650.76, 53.02, 494.03 and 2183.99 hm²; built-up areas will increase at a rate of 3381.79 hm².

The proportion of unused land transferred from 2025-2035 was the highest at approximately 7.41%, with an area that can reach 1951.96 hm². The area of cropland and forest was essentially flat. The area of grassland turned out was up to 1104.40 hm², and the area of grassland turned in was only 453.64 hm²; as such, its performance is reduced. The transfer of built-up areas was only 99.82 hm², while the transfer area was 3481.61 hm², showing an increasing change. The area of water bodies, sandy land and unused land had essentially remained the same; as such, this area had decreased (Appendix Table 3).

According to the spatial distribution there was an increase to the cropland and built-up areas under a

scenario where social benefits were maximized (as per Fig. 4a). Here, cropland increased based on the transformation of other land types from 2025 to 2035; these transformations were distributed in Nugustai, Ganqika, Charisu, Hailutu, and Jinbaotun towns. During this period, the increased built-up area was concentrated in Changsheng, and a small amount of new built-up area was distributed in the south of Ganqika, north of Nugustai, and at the junction of Charisu and Hailutu.

Scenario Simulation of Ecological Benefit Maximization in 2035

In the maximum ecological benefit scenario, cropland, forest, grassland, and unused land were maintained at a scale of 2025. Although cropland did not increase, the decreases in forest land, grassland, and unused land were effectively contained. The built-up area showed a small increase of 547.04 hm², while the areas for water bodies and sandy land experienced a small decrease of 53.02 and 494.03 hm², respectively.

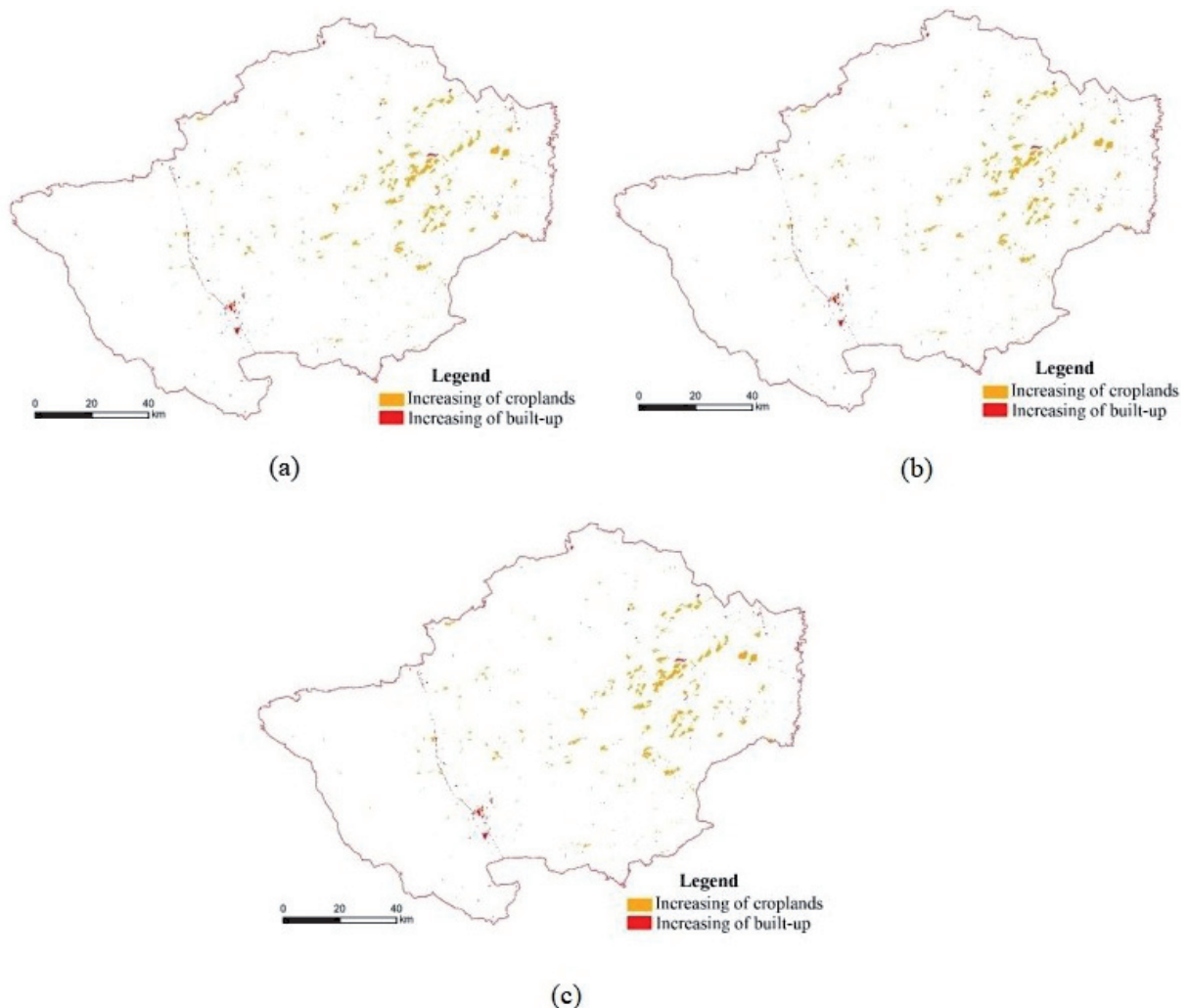


Fig. 4. Spatial distribution of increases to the cropland and built-up areas under the social benefit maximization scenario.

Sandy land had the highest proportion and cropland had the largest area, at 771.69 hm². The area of cropland, forest land, grassland, and unused land were essentially the same. The transferred built-up area was 168.35 hm², and the transferred area was 715.39 hm², indicating an overall increase. The area of water bodies and sandy land only had a small turn area, as demonstrated by the area reduction (Appendix Table 4). Under the premise of the highest ecological benefit, land use scale and spatial land use distribution were closest to the forecasted situation under the current change trend in 2025.

Fig. 4b) shows that when ecological benefits are maximized, there is little change in land use types in terms of space and quantity by 2035. In terms of quantity, the cropland and built-up areas increased slightly. However, there was no spatial concentration change, and their distribution was sporadic within the study area. The cropland increases from other land use type transformations were mainly distributed in Ganqika, and some of the increased cropland was scattered in Nugustai, Changsheng, and Jinbaotun towns. During this period, the increased built-up areas were concentrated in Changsheng, and a small amount of new built-up areas were distributed in the south of Ganqika, the north of Nugustai, and the junction of Charisu and Hailutu. As such, under this ecological benefits scenario, the transformation of other land types to built-up areas was effectively reduced, and considerable areas of forest, grassland, and unused land were reserved. This protects further development space for the Keerqinzuoyihou Banner.

Scenario Simulation of Economic Benefit Maximization in 2035

Under the maximum economic benefit scenario, the proportion of unused land and the grassland were the highest, reaching 19760.76 hm². The area of cropland transferred out was 1283.22 hm², and the area transferred in was 22226.50 hm²; this indicates an overall increase in area. The areas of forest and grassland transferred out were 4225.54 and 19 760.76 hm², and the areas of forest and grassland transferred in were 1517.31 and 874.96 hm², respectively; this indicates a decrease in area. The transferred built-up area was 2460.93 hm², although the transferred area was 5842.72 hm². The area transferred from grassland was the largest (3385.92 hm²), leading to an increase in built-up areas. The trends for water bodies, sandy land, and unused land were similar to those in the social benefit scenario (Appendix Table 5).

Fig. 4c) shows that the spatial layout of cropland and built-up areas increased through the transformation of other land use types from 2025 to 2035. This increase produced a spatial layout similar to the land use change layout under the natural evolution scenario. This demonstrates that the current land use layout in the Keerqinzuoyihou Banner mainly seeks economic

benefits and lacks awareness of socially balanced development and ecological protection.

Conclusions

To optimize spatial land use allocation in the Keerqinzuoyihou Banner, a county-scale CLUE-S model was constructed utilizing current land use data from 2009 to 2017. Spatial land use distribution in the natural evolution scenario in 2025 and the maximization of social, ecological, and economic benefits in 2035 were predicted and simulated. The following conclusions were drawn:

1. In 2009, the land use structure of the Keerqinzuoyihou Banner was dominated by cropland, forest, and grassland, accounting for 22.25%, 15.65%, and 52.09%, respectively, of the study area. Together, these combined land use types accounted for nearly 90% of the total land area. During 2009–2017, the cropland and built-up areas increased rapidly, reaching 271579.49 and 29931.38 hm² respectively, in 2017.
2. The CLUE-S model was used to simulate the spatial land use layout in the Keerqinzuoyihou Banner in 2017. The Kappa coefficient between the simulated results and actual land use was 0.936, indicating that the CLUE-S model is highly accurate and reliable for simulating spatial land use layout in the Keerqinzuoyihou Banner.
3. Under the natural evolution scenarios, the areas of forest, grassland, water bodies, sandy land, and unused land decreased from 2017 to 2025, while cropland and built-up areas increased. When social benefit was maximized, the unused land area was the largest. When ecological benefits were maximized, the proportion of sandy land and cropland area was the highest. When economic benefits were maximized, the proportion of unused land was the highest, and the area of grassland was the largest.
4. The high efficiency and intensification of construction should be taken as the goal at the time of formulating land use policy, so the unreasonable land expansion can be prevented. For this, some measures are proposed as follows, such as considering the growth and decline of urban and rural built-up areas, making the optimization of the layout of built-up areas, as well as achieving the economic sustainable development mode of complementary advantages. In the aspect of ecological land use, the number and spatial distribution of ecologically effective land use such as forest land, cropland and water bodies should be guaranteed. The high standard of basic farmland construction standards and ecological landscape should be used to design and plan the regional ecological land use in advance. The comprehensive playing of its greening role and ecological effect is the design idea, so as to guarantee the food and ecology security.

Acknowledgments

This research was supported by the Natural Science Foundation of Inner Mongolia (Grant NO.2019LH04001) and Fundamental Research Funds for the Inner Mongolia Normal University (NO.2022JBZH012).

Conflict of Interest

The authors declare no conflict of interest.

References

- HONG B., ZHANG P., KE L. Ecological risk assessment and elastic response analysis of land use change in Beijing, China. *Journal of Environmental Protection and Ecology* **19** (3), 1026-1036, **2018**.
- STEHFEST E., VAN ZEIST W.-J., VALIN H., HAVLIK P., POPP A., KYLE P., TABEAU A., MASON-D'CROZ D., HASEGAWA T., BODIRSKY B.L., CALVIN K., DOELMAN J.C., FUJIMORI S., HUMPENOEDER F., LOTZE-CAMPEN H., VAN MEIJL H., WIEBE K. Key determinants of global land-use projections. *Nature Communications* **10**, **2019**.
- XIE H. Towards Sustainable Land Use in China: A Collection of Empirical Studies. *Sustainability* **9** (11), **2017**.
- HENCHIRI M., ALI S., ESSIFI B., KALISA W., ZHANG S., BAI Y. Monitoring land cover change detection with NOAA-AVHRR and MODIS remotely sensed data in the North and West of Africa from 1982 to 2015. *Environmental Science and Pollution Research* **27** (6), 5873, **2020**.
- ZRIBI M., DRIDI G., AMRI R., LILI-CHABAANE Z. Analysis of the Effects of Drought on Vegetation Cover in a Mediterranean Region through the Use of SPOT-VGT and TERRA-MODIS Long Time Series. *Remote Sensing* **8** (12), **2016**.
- DI VITTORIO C.A., GEORGAKAKOS A.P. Land cover classification and wetland inundation mapping using MODIS. *Remote Sensing of Environment* **204**, 1, **2018**.
- SHRESTHA B., YE Q., KHADKA N. Assessment of Ecosystem Services Value Based on Land Use and Land Cover Changes in the Transboundary Karnali River Basin, Central Himalayas. *Sustainability* **11** (11), **2019**.
- FERNANDES SOUZA J.M., DOS REIS E.F., MARTINS A.S., FERREIRA SANTOS A.L. Evaluation of conflict of land use in the Lamarao river watershed, Federal District. *Ciencia Florestal* **29** (2), 950, **2019**.
- BALZTER H., COLE B., THIEL C., SCHMULLIUS C. Mapping CORINE Land Cover from Sentinel-1A SAR and SRTM Digital Elevation Model Data using Random Forests. *Remote Sensing* **7** (11), 14876, **2015**.
- DING J., JIANG Y., LIU Q., HOU Z., LIAO J., FU L., PENG Q. Influences of the land use pattern on water quality in low-order streams of the Dongjiang River basin, China: A multi-scale analysis. *Science of the Total Environment* **551**, 205, **2016**.
- LEI C., WAGNER P.D., FOHRER N. Identifying the most important spatially distributed variables for explaining land use patterns in a rural lowland catchment in Germany. *Journal of Geographical Sciences* **29** (11), 1788, **2019**.
- WANG S.-D., ZHANG H.-B., WANG X.-C. Simulating Land Use Structure Optimization Based on an Improved Multi-Objective Differential Evolution Algorithm. *Polish Journal of Environmental Studies* **28** (2), 887, **2019**.
- WANG G., HAN Q., DE VRIES B. The multi-objective spatial optimization of urban land use based on low-carbon city planning. *Ecological Indicators* **125**, **2021**.
- SHAYGAN M., ALIMOHAMMADI A., MANSOURIAN A., GOVARA Z.S., KALAMI S.M. Spatial Multi-Objective Optimization Approach for Land Use Allocation Using NSGA-II. *Ieee Journal of Selected Topics in Applied Earth Observations and Remote Sensing* **7** (3), 906, **2014**.
- KUMAR N.S., ARUN M. Genetic algorithm-based feature selection for classification of land cover changes using combined LANDSAT and ENVISAT images. *International Journal of Bio-Inspired Computation* **10** (3), 172, **2017**.
- CAO K., LIU M., WANG S., LIU M., ZHANG W., MENG Q., HUANG B. Spatial Multi-Objective Land Use Optimization toward Livability Based on Boundary-Based Genetic Algorithm: A Case Study in Singapore. *Isprs International Journal of Geo-Information* **9** (1), **2020**.
- ZHANG H., ZENG Y., JIN X., SHU B., ZHOU Y., YANG X. Simulating multi-objective land use optimization allocation using Multi-agent system-A case study in Changsha, China. *Ecological Modelling* **320**, 334, **2016**.
- GAO Y., LI Q. A segmented particle swarm optimization convolutional neural network for land cover and land use classification of remote sensing images. *Remote Sensing Letters* **10** (12), 1182, **2019**.
- WANG H., LI W., HUANG W., NIE K. A Multi-Objective Permanent Basic Farmland Delineation Model Based on Hybrid Particle Swarm Optimization. *Isprs International Journal of Geo-Information* **9** (4), **2020**.
- WANG H., WANG M., ZHU Y., NIU J., CHEN X., ZHANG Y. Zoning Permanent Basic Farmland Based on Artificial Immune System coupling with spatial constraints. *Ksii Transactions on Internet and Information Systems* **15** (5), 1666, **2021**.
- HUANG X., XU G., XIAO F. Optimization of a Novel Urban Growth Simulation Model Integrating an Artificial Fish Swarm Algorithm and Cellular Automata for a Smart City. *Sustainability* **13** (4), **2021**.
- WANG J., WANG X., ZHOU S., WU S., ZHU Y., LU C. Optimization of Sample Points for Monitoring Arable Land Quality by Simulated Annealing while Considering Spatial Variations. *International Journal of Environmental Research and Public Health* **13** (10), **2016**.
- LI X., MA X. An improved simulated annealing algorithm for interactive multi-objective land resource spatial allocation. *Ecological Complexity* **36**, 184, **2018**.
- YANG J., SU J., CHEN F., XIE P., GE Q. A Local Land Use Competition Cellular Automata Model and Its Application. *Isprs International Journal of Geo-Information* **5** (7), **2016**.
- FENG Y. Modeling dynamic urban land-use change with geographical cellular automata and generalized pattern search-optimized rules. *International Journal of Geographical Information Science* **31** (6), 1198, **2017**.
- FENG Y., TONG X. Dynamic land use change simulation using cellular automata with spatially nonstationary transition rules. *Giscience & Remote Sensing* **55** (5), 678, **2018**.
- YANG Y.Y., ZHANG S.W., WANG D.Y., YANG J.C., XING X.S. Spatiotemporal Changes of Farming-Pastoral Ecotone in Northern China, 1954-2005: A Case Study in Zhenlai County, Jilin Province. *Sustainability* **7** (1), 1, **2015**.

28. JIANG W.G., CHEN Z., LEI X., JIA K., WU Y.F. Simulating urban land use change by incorporating an autologistic regression model into a CLUE-S model. *Journal of Geographical Sciences* **25** (7), 836, **2015**.
29. MANDAL J., GHOSH N., MUKHOPADHYAY A. Urban Growth Dynamics and Changing Land-Use Land-Cover of Megacity Kolkata and Its Environs. *Journal of the Indian Society of Remote Sensing* **47** (10), 1707, **2019**.
30. SONG W., CHEN B.M., ZHANG Y. Land-use change and socio-economic driving forces of rural settlement in China from 1996 to 2005. *Chinese Geographical Science* **24** (5), 511, **2014**.
31. LIU C., XU Y.Q., SUN P.L., HUANG A., ZHENG W.R. Land use change and its driving forces toward mutual conversion in Zhangjiakou City, a farming-pastoral ecotone in Northern China. *Environmental Monitoring and Assessment* **189** (10), **2017**.
32. DU X.J., HUANG Z.H. Ecological and environmental effects of land use change in rapid urbanization: The case of Hangzhou, China. *Ecological Indicators* **81**, 243, **2017**.
33. LIU F., ZHENG X.Q., HUANG Q. Predictive Measurement of the Structure of Land Use in an Urban Agglomeration Space. *Sustainability* **10** (1), **2018**.
34. VULEVIC T., TODOSIJEVIC M., DRAGOVIC N., ZLATIC M. Land use optimization for sustainable development of mountain regions of western Serbia. *Journal of Mountain Science* **15** (7), 1471, **2018**.
35. TURK E., ZWICK P.D. Optimization of land use decisions using binary integer programming: The case of Hillsborough County, Florida, USA. *Journal of Environmental Management* **235**, 240, **2019**.
36. LI Q., WANG L., ZHU Y., MU B., AHMAD N. Fostering land use sustainability through construction land reduction in China: an analysis of key success factors using fuzzy-AHP and DEMATEL. *Environmental Science and Pollution Research*, **2021**.
37. BAO G.Y., HUANG H., GAO Y.N., WANG D.B. Study on Driving Mechanisms of Land Use Change in the Coastal Area of Jiangsu, China. *Journal of Coastal Research*, 104, **2017**.
38. RAHNAMA M.R. Forecasting land-use changes in Mashhad Metropolitan area using Cellular Automata and Markov chain model for 2016-2030. *Sustainable Cities and Society* **64**, **2021**.

Appendix

Table 1. Land use probability transfer matrix from 2009 to 2017.

2009 \ 2017	Cropland	Forest land	Grassland	Built-up	Water bodies	Sandy land	Unused land
Cropland	99.82%	0	0	0.18%	0	0	0
Forest	0.95%	98.73%	0	0.32%	0	0	0
Grassland	2.06%	0	97.65%	0.26%	0.01%	0	0.01%
Built-up	0.01%	0	0	99.99%	0	0	0
Water bodies	0.35%	0	0	0.05%	99.60%	0	0
Sandy land	0.47%	0	0	0.06%	0	99.46%	0
Unused land	6.14%	0	0	0.50%	0	0	93.36%

Table 2. Land use probability transfer matrix table from 2017 to 2025.

2017 \ 2025	Cropland	Forest	Grassland	Built-up	Water bodies	Sandy land	Unused land
Cropland	99.63%	0.09%	0.13%	0.13%	0.01%	0	0
Forest	1.74%	98.05%	0.14%	0.07%	0	0	0
Grassland	2.09%	0.10%	97.33%	0.46%	0.01%	0.01%	0.01%
Built-up	5.44%	0.18%	0.07%	94.26%	0.01%	0.02%	0.02%
Water bodies	1.07%	0	0.16%	0.06%	98.69%	0	0.01%
Sandy land	0.81%	0.02%	0.10%	0.04%	0	99.03%	0
Unused land	2.03%	0.10%	0.17%	4.23%	0.01%	0	93.46%

Table 3. Land use probability transfer matrix under social benefit maximization scenario in 2025–2035.

2025 \ 2035	Cropland	Forest	Grassland	Built-up	Water bodies	Sandy land	Unused land
Cropland	99.56%	0.02%	0.17%	0.25%	0	0	0
Forest	0.03%	99.92%	0.02%	0.03%	0	0	0
Grassland	0.03%	0.01%	99.81%	0.15%	0	0	0
Built-up	0.13%	0.06%	0.09%	99.70%	0	0.02%	0
Water bodies	0.15%	0	0.06%	0.04%	99.76%	0	0
Sandy land	0.89%	0.01%	0.07%	0.01%	0	99.02%	0
Unused land	0.13%	0.02%	0.12%	7.14%	0	0	92.60%

Table 4. Land use probability transfer matrix table under the maximizing ecological benefit scenario from 2025 to 2035.

2025 \ 2035	Cropland	Forest	Grassland	Built-up	Water bodies	Sandy land	Unused land
Cropland	99.74%	0.03%	0.13%	0.10%	0	0	0
Forest	0.04%	99.93%	0.01%	0.01%	0	0	0
Grassland	0.02%	0	99.93%	0.04%	0	0	0
Built-up	0.10%	0.03%	0.05%	99.50%	0	0	0.31%
Water bodies	0.10%	0	0.03%	0.03%	99.83%	0	0
Sandy land	1.47%	0.01%	0.10%	0.08%	0	98.35%	0
Unused land	0.01%	0.01%	0.02%	0	0	0	99.95%

Table 5. Land use probability transfer matrix under the maximizing economic benefits scenario from 2025 to 2035

2025 \ 2035	Cropland	Forest	Grassland	Built-up	Water bodies	Sandy land	Unused land
Cropland	99.57%	0.13%	0.17%	0.12%	0	0	0
Forest	2.13%	97.59%	0.18%	0.09%	0	0	0
Grassland	2.69%	0.13%	96.54%	0.59%	0.01%	0.02%	0.01%
Built-up	7.10%	0.23%	0.08%	92.56%	0	0	0.02%
Water bodies	1.05%	0	0.13%	0.08%	98.73%	0	0
Sandy land	1.39%	0.01%	0.20%	0.04%	0	98.36%	0
Unused land	2.46%	0.05%	0.19%	5.38%	0	0.01%	91.90%

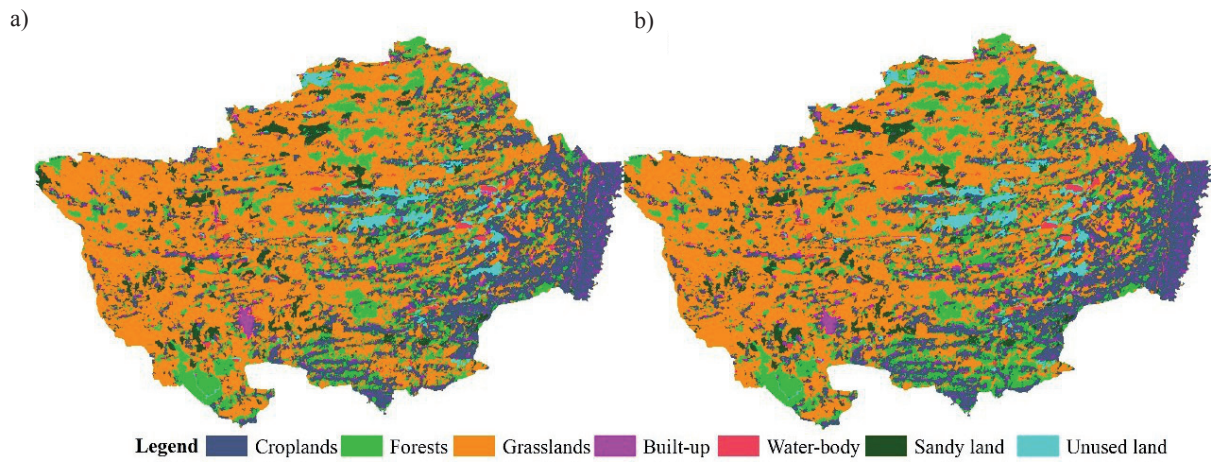


Fig. 1. Land use status in 2017: a) simulation and b) results.